JOURNAL OF VIROLOGY, Oct. 2006, p. 10208–10217 Vol. 80, No. 20
0022-538X/06/$08.00+0 doi:10.1128/JVI.00062-06

Murine Model for Dengue Virus-Induced Lethal Disease with Increased Vascular Permeability

Sujan Shresta,[2]* Kristin L. Sharar,[2]† Daniil M. Prigozhin,[2]† P. Robert Beatty,[1] and Eva Harris[1]*

Division of Infectious Diseases, School of Public Health, 140 Warren Hall, University of California at Berkeley, Berkeley, California 94720-7360,[1] and La Jolla Institute for Allergy and Immunology, 10355 Science Center Drive, San Diego, California 92121[2]

Received 9 January 2006/Accepted 31 July 2006

Lack of an appropriate animal model for dengue virus (DEN), which causes dengue fever and dengue hemorrhagic fever/dengue shock syndrome (DHF/DSS), has impeded characterization of the mechanisms underlying the disease pathogenesis. The cardinal feature of DHF/DSS, the severe form of DEN infection, is increased vascular permeability. To develop a murine model that is more relevant to DHF/DSS, a novel DEN strain, D2S10, was generated by alternately passaging a non-mouse-adapted DEN strain between mosquito cells and mice, thereby mimicking the natural transmission cycle of the virus between mosquitoes and humans. After infection with D2S10, mice lacking interferon receptors died early without manifesting signs of paralysis, carried infectious virus in both non-neuronal and neuronal tissues, and exhibited signs of increased vascular permeability. In contrast, mice infected with the parental DEN strain developed paralysis at late times after infection, contained detectable levels of virus only in the central nervous system, and displayed normal vascular permeability. In the mice infected with D2S10, but not the parental DEN strain, significant levels of serum tumor necrosis factor alpha (TNF-α) were produced, and the neutralization of TNF-α activity prevented early death of D2S10-infected mice. Sequence analysis comparing D2S10 to its parental strain implicated a conserved region of amino acid residues in the envelope protein as a possible source for the D2S10 phenotype. These results demonstrate that D2S10 causes a more relevant disease in mice and that TNF-α may be one of several key mediators of severe DEN-induced disease in mice. This report represents a significant advance in animal models for severe DEN disease, and it begins to provide mechanistic insights into DEN-induced disease in vivo.

Dengue virus (DEN) causes dengue fever (DF) and dengue hemorrhagic fever/dengue shock syndrome (DHF/DSS), with an estimated 2.5 billion people at risk for infection in subtropical and tropical regions of the world (6). DEN is a positive-sense, single-stranded RNA virus that belongs to the family *Flaviviridae* and the genus *Flavivirus*, which includes yellow fever (YFV), West Nile, Japanese encephalitis, and St. Louis encephalitis viruses. Primary infection with any one of the four DEN serotypes typically leads to DF, a debilitating but self-limited acute febrile illness. However, some primary infections and a larger percentage of secondary infections with a different serotype result in the severe, life-threatening DHF/DSS, characterized by increased vascular permeability and hemorrhagic manifestations (6). Despite its name, bleeding manifestations are minor and major hemorrhages are unusual; instead, increased vascular permeability is the hallmark of DHF/DSS. In rare cases of DHF/DSS, neurologic abnormalities, including encephalitis, may also occur (32). DEN is transmitted to humans by the mosquitoes *Aedes aegypti* and *Aedes albopictus*. Due to uncontrolled urbanization, globalization, and dissemination of DEN-transmitting mosquitoes, the frequency of DEN epidemics has increased and DHF/DSS has spread (22). Currently, DEN is a major public health problem throughout the world, yet DEN-specific therapies and vaccines are unavailable.

Despite global morbidity and mortality, DEN pathogenesis is poorly understood. Numerous studies suggest that DHF/DSS may be an immunopathogenic disease (11, 18, 27, 28). Specifically, epidemiologic studies have shown that secondary infection with a heterologous DEN serotype is a major risk factor for the development of DHF/DSS. Two non-mutually exclusive mechanisms have been proposed to explain how secondary DEN infections may enhance disease severity. First, the ADE ("antibody-dependent enhancement") hypothesis postulates that DEN serotype-cross-reactive antibodies (Abs) at non-neutralizing conditions contribute to DHF/DSS by increasing infection of Fcγ receptor-positive cells, such as monocytes and macrophages (5, 12), leading to an increase in viremia, which is correlated with more-severe disease (35). Second, the "aberrant T-cell response" hypothesis proposes that the reactivation of serotype-cross-reactive memory T cells during secondary infection results in abnormal T-cell activation and cytokine release or apoptosis (25, 27). At present, the exact mechanisms by which either the ADE phenomenon or inappropriate cellular immune response contributes to DHF/DSS are undefined. Besides the host immune status, DEN strains themselves may influence the

* Corresponding author. Mailing address for Sujan Shresta: Division of Vaccine Discovery, La Jolla Institute for Allergy and Immunology, 9420 Athena Circle, La Jolla, CA 92037. Phone: (858) 752-6944. Fax: (858) 752-6987. E-mail: sujan@liai.org. Mailing address for Eva Harris: Division of Infectious Diseases, School of Public Health, 140 Warren Hall, University of California at Berkeley, Berkeley, CA 94720-7360. Phone: (510) 642-4845. Fax: (510) 642-6350. E-mail: eharris@berkeley.edu.

† These authors contributed equally.

disease severity in humans with either primary or secondary DEN infection (7, 8, 19). Taken together, accumulating evidence implies that both viral and host factors contribute to DEN pathogenesis.

Although clinical and experimental observations in vitro have provided valuable insights into DEN-host interactions, the roles of viral and host factors in regulating DEN-induced disease in vivo are yet to be elucidated. In particular, the mechanisms by which DEN infection leads to increased vascular permeability, the cardinal feature of DHF/DSS and the cause of shock, remain unclear, and this is mainly due to the lack of a suitable animal model. Therefore, as a first step towards investigating the molecular basis of DEN-induced disease, the present work seeks to develop a murine model of DEN disease that better reflects the human disease. Unlike existing murine models in which paralysis is the dominant clinical phenotype, here we report a mouse model of DEN disease in which the infected animals exhibit increased vascular permeability and fatal non-neurological disease.

MATERIALS AND METHODS

Mice. 129/Sv mice doubly deficient in alpha/beta interferon (IFN-α/β) and IFN-γ receptors (AG129) were obtained from Herbert Virgin (Washington University School of Medicine, St. Louis, MO). They were bred and maintained under specific-pathogen-free conditions at the animal facility at the University of California, Berkeley (UC Berkeley) or at the La Jolla Institute for Allergy and Immunology (LIAI). All experiments were approved by the Animal Care and Use Committee at UC Berkeley and the Animal Care Committee at LIAI. Age- and sex-matched mice 5 to 6 weeks of age were used, and experimental groups contained three to six animals.

Tissue culture and viruses. All reagents for tissue culture were endotoxin low, and cell lines were routinely tested for mycoplasma contamination. The parental PL046 DEN virus (Taiwanese isolate; *Aedes albopictus* C6/36 cell culture adapted) was originally obtained from Huan-Yao Lei (National Cheng Kung University, Taiwan). Stocks of PL046 were amplified in C6/36 cells, concentrated via ultracentrifugation, and titrated by plaque assays using BHK-21 cells, as previously described (29). To generate D2S10, a single AG129 mouse was intravenously injected with 10^8 PFU of PL046, followed by harvesting of serum at day 3 postinfection (d3 p.i.). The mouse was euthanized by isoflurane inhalation just prior to obtaining whole blood via cardiac puncture. The virus in the serum was amplified in C6/36 cells for 7 days and concentrated by ultracentrifugation, and approximately 10^5 to 10^6 PFU of the C6/36 cell-amplified virus was intravenously injected into another naive AG129 mouse. This entire procedure was repeated 10 times to obtain D2S10 stocks. To generate a sufficient quantity of virus for performing all of the experiments in this study, the D2S10 stock was passaged one or two more times in C6/36 cells. For some control experiments, D2S10 was inactivated by UV irradiation at 320 nm for 20 min at a distance of 5 cm. All virus preparations used for these studies were concentrated 30- to 50-fold by ultracentrifugation (starting volume, 60 to 100 ml; ending volume, 1 to 2 ml), and the titers of the centrifuged virus were determined after one freeze-thaw cycle at −80°C.

Quantitation of virus in infected mice. Mice were euthanized by isoflurane inhalation, and blood was collected after cardiac puncture for isolation of serum. Mice were then perfused with 30 to 50 ml phosphate-buffered saline (PBS), and tissue samples were harvested, processed, and tested for the presence of infectious virus by plaque assay in BHK-21 cells, as previously described (29). The limit of the sensitivity of the plaque assay was 100 PFU/ml or g of tissue weight.

Quantitation of vascular permeability. Vascular leakage was examined by intravascular administration of Evans blue (Sigma-Aldrich) as described previously (34). In brief, Evans blue (0.2 ml of 0.5% solution in PBS) was injected intravenously into PL046- or D2S10-infected mice between d3 to d4 p.i., when D2S10-infected mice began to exhibit signs of illness, such as ruffled fur, hunched posture, and lethargy. After 2 h, the mice were euthanized and extensively perfused with PBS, and then tissues were harvested and placed into preweighed tubes containing formamide (Sigma-Aldrich). Samples were incubated at 37°C for 24 h, and then Evans blue concentrations in formamide extracts were quantitated by measuring absorbances at 610 nm. Data were expressed as optical density at 610 nm per g of tissue weight.

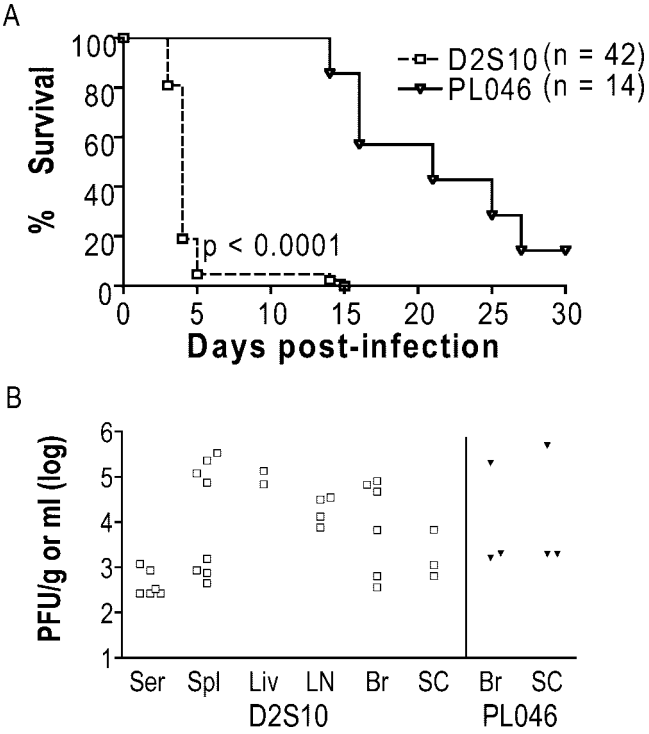

FIG. 1. Susceptibility of AG129 mice to infection with DEN2 strain D2S10 or PL046. Mice were intravenously inoculated with 10^7 PFU of D2S10 or the parental PL046 strain and monitored daily until d30 p.i. Mice that exhibited morbidity or paralysis were immediately euthanized. (A) Kaplan-Meier survival curves. Data from three to six independent experiments were pooled, and the *P* value between D2S10 and PL046 is indicated. Approximately 3 to 10 times more viral RNA was present per PFU of D2S10 than per PFU of PL046; *n*, total number of mice per group. (B) Viral burden in tissues. Levels of infectious virus in the serum (Ser), spleen (Spl), liver (Liv), lymph nodes (LN), brain (Br), and spinal cord (SC) from D2S10-infected moribund mice on d4 to d5 p.i. and PL046-infected mice with paralysis on d16 to d27 p.i. were quantitated by standard plaque assay. Each symbol represents an individual mouse. Open symbols, D2S10-infected mice; filled symbols, PL046-infected mice.

Histopathology. For histologic studies, mice were euthanized and tissues were immediately harvested and fixed in 10% buffered formalin. Fixed tissues were paraffin embedded, sectioned, and stained with hematoxylin and eosin by the BioPathology Sciences, South San Francisco, Calif.

Measurement of TNF-α. A standard sandwich enzyme-linked immunosorbent assay (ELISA) was performed to quantitate the levels of tumor necrosis factor alpha (TNF-α) in the serum and supernatants of tissue homogenates. A mouse TNF-α ELISA Ready-SET-Go kit (eBioscience) was used according to the manufacturer's instructions. The optical density at 450 nm of each sample was measured using a Bio-Tek El_x808 microplate reader (Bio-Tek Instruments) and KCjunior software (Bio-Tek Instruments). TNF-α levels were expressed as the number of picograms per ml or g of tissue weight. The limit of detection of TNF-α was 15 pg/ml.

Neutralization of TNF-α. TNF-α in D2S10-infected mice was depleted by intraperitoneally injecting 100 μg of purified, functional grade (i.e., azide-free, sterile-filtered, and with endotoxin levels of <0.001 ng/μg) anti-mouse TNF-α (clone MP6-XT3; eBioscience) on d1, d2, and d3 p.i. Control animals were treated with functional grade, purified rat immunoglobulin G1 isotype control (eBioscience).

Nucleotide sequence analysis. Viral RNA was isolated using an RNeasy Mini kit (QIAGEN), and the genome was amplified by real-time reverse transcription (RT)-PCR with previously described primers (9) using SuperScript III and high-fidelity *Pfu* Turbo polymerase (Invitrogen). Automated sequencing was performed at the UC Berkeley sequencing facility. For determination of consensus

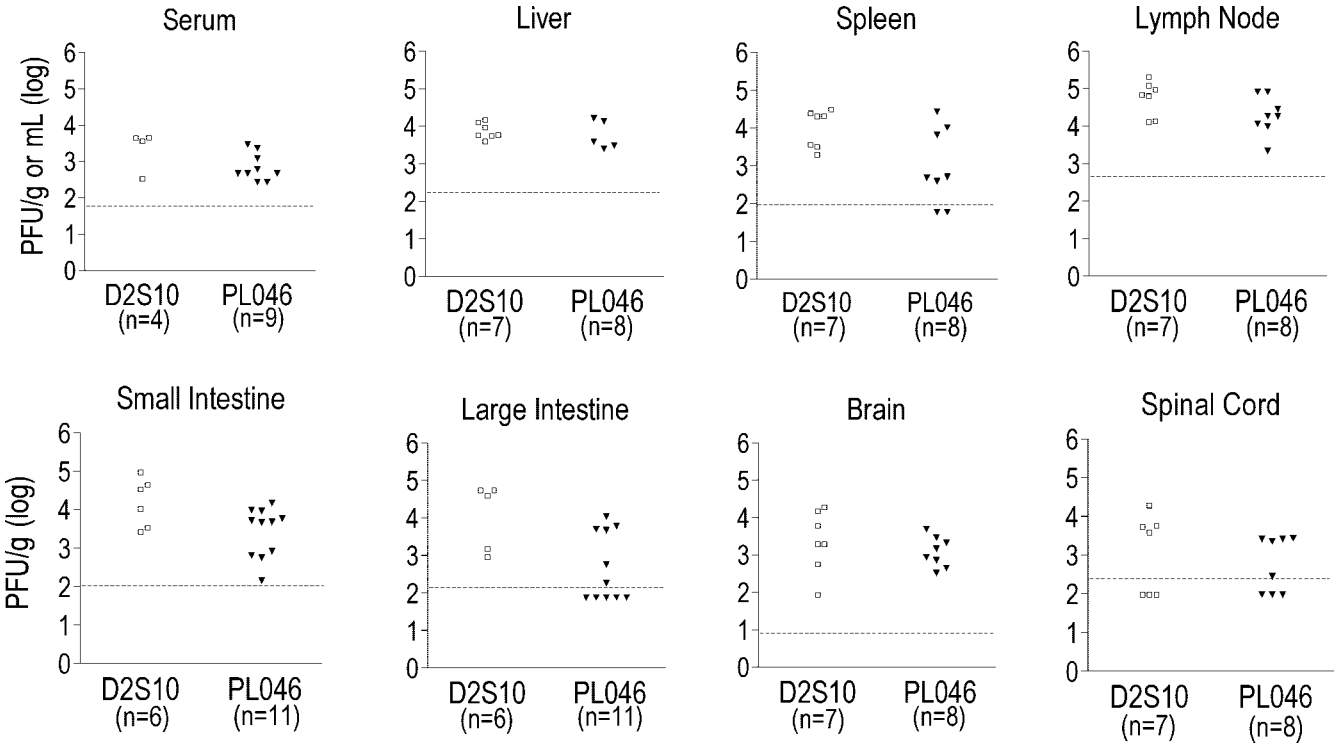

FIG. 2. Viral titers in tissues of D2S10- or PL046-infected AG129 mice at d3 p.i. AG129 mice were intravenously infected with 10^7 PFU of the D2S10 or PL046 strain and euthanized 3 days after infection. Tissues were harvested, and DEN titers were determined by plaque assay. Data from two to three separate experiments are shown. Each symbol represents an individual mouse in which virus was detected; *n*, total number of mice; open symbols, D2S10-infected mice; closed symbols, PL046-infected mice. Discrepancies between the number of symbols and *n* indicate that some infected mice do not contain detectable levels of infectious DEN.

sequence, PCR products were directly sequenced in both directions using the PCR primers, and the 5′ and 3′ termini were sequenced using an RLM-RACE kit (Ambion). Two independent experiments per virus stock (starting with RNA isolation) were conducted to exclude the contribution of real-time RT-PCR artifacts. Sequences were evaluated using 4Peaks software (http://mekentosj.com/4peaks/), and sequence assembly and analysis were performed using Gene Jockey II (Biosoft). For sequence analysis of individual clones, fragments corresponding to amino acid residues 92 to 283 of domain II of the envelope (E) protein were PCR amplified, cloned into pCR2.1-Topo vector (Invitrogen), and amplified in DH5α competent cells. A total of 34 PL046 and 43 D2S10 clones were sequenced.

Statistical analysis. All statistical analyses were performed using GraphPad Prism software, version 4.0a (GraphPad Prism). Kaplan-Meier survival curves were analyzed by the log rank test. For viral burden analysis, an unpaired *t* test with Welch's correction was used. To examine the vascular permeability and TNF-α levels, one-way analysis of variance with Tukey's multiple comparison test was performed. Values were considered significant at a P of <0.05.

RESULTS

D2S10 is a highly virulent DEN strain that causes a fatal non-neurological disease in mice. As part of our ongoing efforts towards developing a murine model of DEN disease that is more relevant to human illness, we generated a new DEN strain by alternately passaging a non-mouse-adapted DEN strain between mosquito cells and mice. Specifically, PL046, a Taiwanese DEN serotype 2 (DEN2) human isolate that is mosquito cell culture adapted, was intravenously injected into doubly deficient 129/Sv mice lacking receptors for IFN-α/β and IFN-γ (*Ifnar1*$^{-/-}$ and *Ifngr1*$^{-/-}$; hereafter referred to as AG129 mice), followed by the harvest of serum on d3 p.i. Virus in the serum was amplified in mosquito cells and then intravenously injected into another AG129 mouse. After repeating this process a total of 10 times, we obtained strain D2S10. At 10^7 PFU, D2S10 caused a lethal infection in AG129 mice between d3 to d5 p.i. (Fig. 1A), although it did not establish infection in wild-type mice (data not shown). The infected AG129 mice exhibited hunched posture, ruffled fur, and lethargy, but no paralysis. This phenotype was unchanged by the treatment of D2S10-infected AG129 mice with sulfamethoxazole/trimethoprim antibiotic suspension (200 mg/40 mg/5 ml added to drinking water immediately after infection), eliminating the possibility that the observed phenotype was due to bacterial sepsis and supporting a direct role for the virus in causing disease. Only 5% of D2S10-infected AG129 mice remained healthy at d5 p.i., and all of them succumbed to infection by d14 p.i. In contrast, AG129 mice that were infected with the parental DEN2 PL046 strain did not show any signs of illness except for paralysis starting at d14 p.i. Approximately 14% of PL046-infected mice remained free from disease until the end of the experiments at d30 p.i. As expected, the paralytic mice harbored infectious virus only in the brain and spinal cord, whereas the moribund D2S10-infected mice contained infectious DEN in both neuronal and non-neuronal tissues, including the serum, liver, lymph node, and spleen (Fig. 1B). To confirm that the D2S10-induced phenotype was due to the virus and not other factors in the inoculum, mice were infected with D2S10 that was treated with neutralizing anti-DEN2

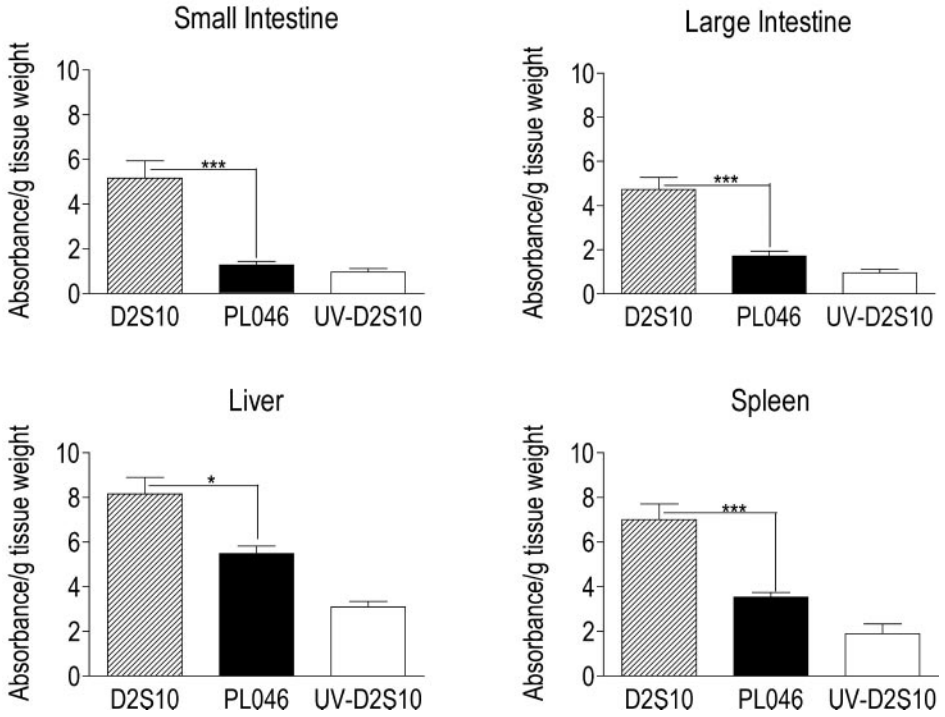

FIG. 3. Vascular leakage in tissues of D2S10-infected AG129 mice. AG129 mice were intravenously inoculated with 10^7 PFU of D2S10 (hatched bar), PL046 (black bar), or UV-irradiated D2S10 (white bar). At d3 p.i., when D2S10-infected mice began to exhibit clinical signs of illness, mice were administered intravenous Evans blue (0.2 ml of 0.5% in PBS per mouse). After 2 h, mice were euthanized and flushed extensively with PBS, and then tissues were harvested. Evans blue concentrations were quantified after formamide extraction by measuring absorbance at 610 nm. Data are expressed as means ± standard deviations of Evans blue optical density/g of wet tissue and are pooled from two to three independent experiments. Total numbers of mice per group are as follows: 14 for D2S10, 11 for PL046, and 4 for UV-D2S10. Asterisks indicate differences that are statistically significant between D2S10- and PL046-infected mice (*, $P < 0.05$; ***, $P < 0.001$).

(clone 3H5; 0.5 mg/ml of purified immunoglobulin G) Ab for 2 h at 37°C. 3H5 neutralization reduced the initial titer of D2S10 (10^7 PFU) to approximately 10^5 PFU. Mice infected with 3H5-neutralized D2S10 began to develop paralysis starting at d20 p.i.; in contrast, mice that were infected with non-neutralized D2S10 (10^7 PFU) died by d5 p.i. without paralysis. At a lower viral dose (10^6 PFU), D2S10 did not cause a lethal infection in AG129 mice; instead, D2S10-infected AG129 mice manifested paralysis at a significantly faster rate than did PL046-infected animals and contained detectable levels of DEN only in the brain and spinal cord (data not shown). These results indicate that D2S10 is more virulent than PL046 in vivo and can cause a nonparalytic lethal disease in mice.

To begin to understand D2S10-induced disease, the levels of infectious virus were examined in AG129 mice 3 days after infection with 10^7 PFU of D2S10 or PL046. At this time point, the majority of D2S10-infected mice were alive and were beginning to display ruffled fur, hunched posture, and lethargy, whereas PL046-infected mice appeared completely healthy. Both D2S10- and PL046-infected mice contained infectious virus in several tissues such as the serum, spleen, and large intestine (Fig. 2). Differences in viral titers between D2S10- and PL046-infected mice, as measured by plaque assay, were not statistically significant. Approximately 3 to 10 times more viral RNA was present per PFU of D2S10 than per PFU of PL046 (data not shown); however, mice that were infected with 10^8 PFU of PL046 developed only paralysis (30, 31), indicating that injection of mice with higher PL046 viral copy numbers does not convert the paralytic phenotype into a more lethal, D2S10-like disease.

D2S10 induces increased vascular permeability in mice. The presence of the fatal non-neurologic disease in D2S10-infected AG129 mice suggested that D2S10 might cause a phenotype in these mice more relevant to the human disease. Therefore, we asked whether D2S10 induced increased vascular permeability, the key feature of severe DEN infection in humans. To assess the integrity of the vascular endothelial barrier, DEN-infected AG129 mice were intravenously injected with Evans blue, a dye that preferentially binds to proteins such as albumin, and the extravasation of the dye into tissues was quantitated spectrophotometrically. Between d3 to d4 p.i., when all D2S10-infected mice exhibited clinical signs of illness but none of the animals inoculated with PL046 or UV-irradiated D2S10 were ill, D2S10-infected mice had significantly higher amounts of Evans blue in the small intestine, large intestine, liver, and spleen than did the other two groups (Fig. 3). Tissues such as the lungs, lymph nodes, brains, and spinal cords of D2S10-infected mice contained low levels of Evans blue, similar to control animals injected with PL046 or UV-irradiated D2S10 (data not shown). These data indicate that D2S10, but not PL046 or UV-irradiated D2S10, induces increased vascular permeability in certain tissues of the infected mice.

To assess vascular leakage in D2S10-infected AG129 mice further, we next performed histologic analysis by examining

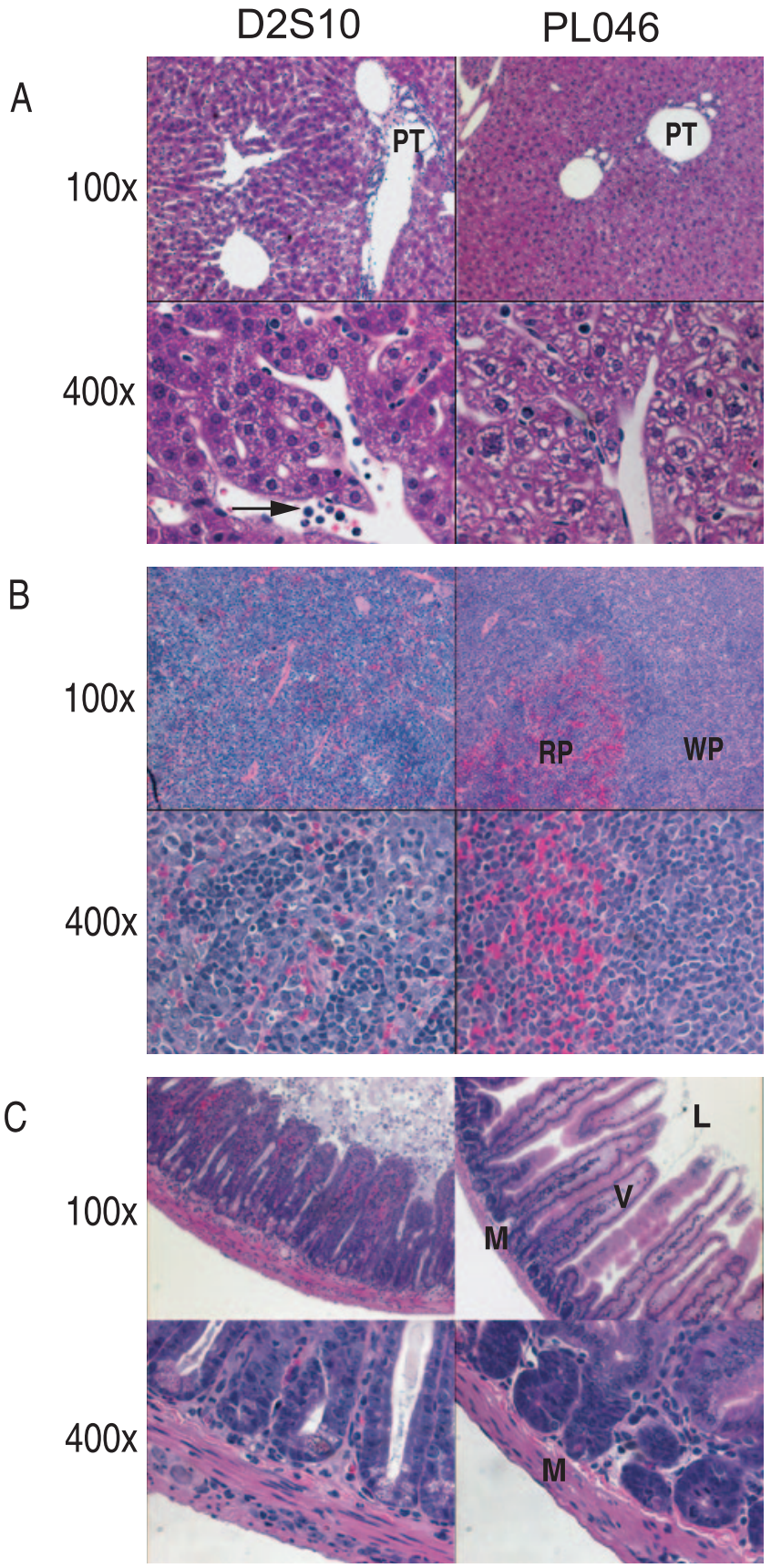
D2S10
PL046
A
100x
400x
PT
PT
B
100x
400x
RP
WP
C
100x
400x
L
V
M
M

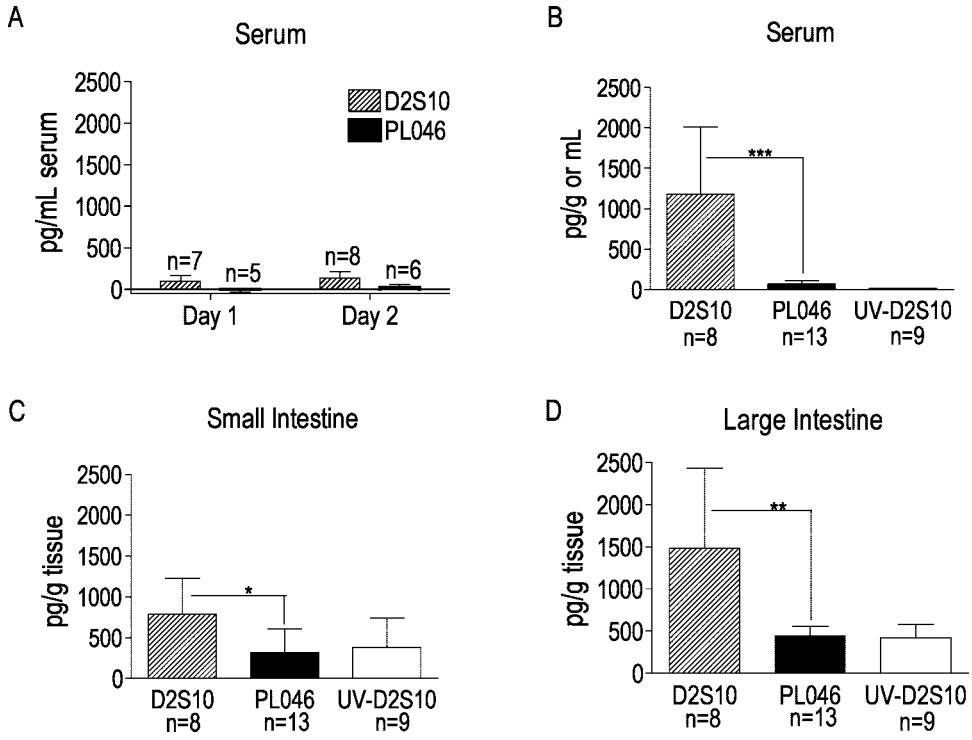

FIG. 5. TNF-α production in D2S10-infected AG129 mice. AG129 mice were inoculated with 10^7 PFU of D2S10 (hatched bars), PL046 (black bars), or UV-irradiated D2S10 (white bars) and sacrificed on d1, d2, or d3 p.i. TNF-α levels in the serum on d1 and d2 p.i. (A) and in the serum (B), small intestine (C), and large intestine (D) on d3 p.i. were analyzed by ELISA. Results represent the mean values ± standard deviations; *n*, number of mice per group. Asterisks indicate differences that are statistically significant (*, $P < 0.05$; **, $P < 0.01$; ***, $P < 0.001$).

hematoxylin and eosin-stained tissue sections from the livers, spleens, and intestinal tracts of D2S10- or PL046-infected mice between d3 and d4 p.i. Samples from PL046-infected mice demonstrated normal liver, spleen, and intestine histology; in contrast, sections of all three tissues from D2S10-infected mice revealed damage at the cellular and tissue levels (Fig. 4). Specifically, in D2S10-infected mice, (i) liver sections contained inflammatory infiltrates in the portal triad and hepatocytes that were dilated and multivesicular, with a vacuolated appearance (Fig. 4A), (ii) spleen sections showed mononuclear cell infiltrates and dead cells (Fig. 4B), and (iii) samples throughout the intestinal tract revealed cellular debris in the lumen, destruction of the columnar epithelium, and a thickening of the mucosal layer due to the presence of inflammatory cells (Fig. 4C). These histologic findings provide evidence for pathological changes in the tissues that exhibit signs of increased vascular permeability in D2S10-infected mice, and they suggest an association between inflammatory infiltrates and interstitial leakage. Taken together, the Evans blue data and histopathologic observations support the conclusion that D2S10-infected AG129 mice manifest increased vascular permeability, a hallmark of DHF/DSS.

Neutralization of TNF-α in AG129 mice prevents D2S10-induced early lethality. The presence of inflammatory infiltrates in tissues of D2S10-infected AG129 mice suggested a role for inflammatory responses in causing D2S10-induced pathology and the early deaths of infected mice. Indeed, numerous human studies have suggested that proinflammatory cytokines may be involved in the pathogenesis of DHF/DSS. In particular, TNF-α has been detected more frequently and at higher levels in the serum of patients with DHF/DSS than in those with DF (10, 13, 17). Therefore, we investigated whether TNF-α may be responsible for causing D2S10-induced death by measuring TNF-α levels in AG129 mice that had been injected with 10^7 PFU of D2S10 or PL046 by ELISA. On d1 and d2 p.i., little or no TNF-α was detected in the serum of PL046-infected mice, whereas small amounts of this cytokine were observed in the serum of D2S10-infected mice (Fig. 5A). By d3 p.i., significantly higher levels of TNF-α were present in the serum and supernatants of intestinal tract homogenates of

FIG. 4. Pathology of D2S10-induced tissue damage in AG129 mice. Representative hematoxylin and eosin sections from the liver (panel A), spleen (panel B), and small intestine (panel C) of AG129 mice that were intravenously infected with 10^7 PFU of D2S10 (images on the left) or PL046 (images on the right) at d3 p.i. are shown. Samples from at least three independent experiments were reviewed. For each panel, photographs were taken at 100× (top row) or 400× (bottom row). (A) PT, portal triad; the arrow shows inflammatory cells. (B) WP, white pulp; RP, red pulp. Note the replacement of red pulp by inflammatory cells in D2S10-infected mice. (C) L, lumen; V, villus; M, muscular layer. Note cell debris in the lumen and inflammatory infiltrates in the muscular layer of D2S10-infected samples.

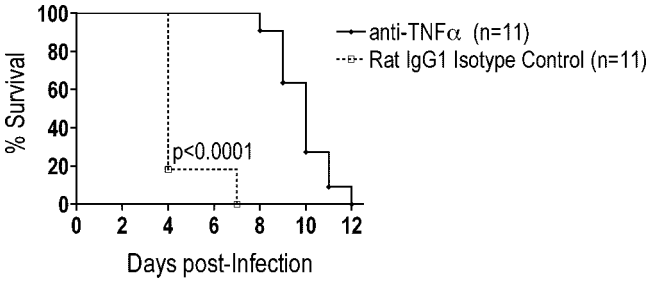

FIG. 6. Survival of D2S10-infected AG129 mice after treatment with anti-TNF-α. AG129 mice were inoculated with 10^7 PFU of D2S10, followed by the intraperitoneal injection of anti-TNF-α or isotype control Ab on days 1, 2, and 3 after infection. Infected mice were followed daily for lethality or paralysis. All isotype control-treated mice succumbed to infection without exhibiting signs of paralysis, whereas all anti-TNF-α-injected mice developed paralysis. As per our animal protocol, mice with paralysis were immediately euthanized. The paralyzed mice were scored as death for Kaplan-Meier survival curve analysis. Data were pooled from three separate experiments; *n*, total number of mice per group; the *P* value is indicated.

D2S10-infected AG129 mice compared to levels in PL046-infected or UV-irradiated D2S10-injected mice (Fig. 5B-D), suggesting a role for TNF-α in the pathogenesis of disease in D2S10-infected mice.

Next, D2S10-infected AG129 mice were administered 100 μg of anti-mouse TNF-α or isotype control Ab intraperitoneally on d1, d2, and d3 p.i. Neutralization of TNF-α binding and biological activity significantly prevented the lethal infection between d3 and d5 p.i. and instead resulted in the development of paralysis at later time points p.i. (Fig. 6). As expected, the isotype control Ab-treated group died early after infection, without exhibiting signs of paralysis. These results demonstrate that TNF-α is responsible for causing early lethality in AG129 mice with D2S10 infection.

Molecular analysis of D2S10. To identify viral determinants responsible for this TNF-α-induced early lethality, consensus sequence analysis was performed on cDNA derived from the RNA genomes of the parental virus and D2S10. Seven nucleotide changes occurred between PL046 and D2S10 coding regions, with one of these resulting in an amino acid substitution (Lys to Glu) at position 128 within domain II of the major envelope glycoprotein E (Table 1). Only one nucleotide change at position 10,564 was identified within the untranslated regions (UTR) of the two viruses. Further examination of the primary sequencing files suggested that the region surrounding the E protein residue 128 in D2S10 might be more heterogeneous than in PL046. Therefore, 30 to 40 clones of this particular segment of either D2S10 or PL046 was amplified by real-time RT-PCR, cloned into a Topo vector, and sequenced. Table 2 shows that 27 out of 34 clones derived from the parental virus matched the consensus PL046 amino acid sequence, and only 7 out of 34 clones differed at amino acid positions 150, 153, or 173 of the E protein. In contrast, the same region within the E protein of D2S10 contained a higher frequency of amino acid substitutions. All 43 clones contained a charge change mutation, and changes at eight residues were found in D2S10: 122 (Lys→Ile), 124 (Asn→Asp/Ile), 126 (Lys→Glu), 128 (Lys→Glu), 130 (Val→Met), 222 (Pro→Ala), 228 (Gly→Glu), and 229 (Ser→Leu) (Table 3). Based on the published DEN2 E protein structure, these residues in PL046 formed part of a basic patch on the external surface of the protein at the base of domain II, near the region postulated to affect fusion activity (23, 26). These positively charged residues, which have been identified in other DEN2 strains and speculated to bind heparan sulfate (24), became more negatively charged amino acids in D2S10. These observations suggest that the DEN2 E protein, especially the basic patch on domain II, may be an important site for mutations that enhance virulence in vivo.

TABLE 1. Consensus sequence analysis of PL046 and D2S10

Genomic position	Nucleotide		Amino acid[a]		Protein position
	PL046	D2S10	PL046	D2S10	
345	G	C	Gly	Gly	
1318	A	G	Lys	**Glu**	E no. 128
2823	A	C	Leu	Leu	
9201	A	G	Leu	Leu	
9207	T	C	Asp	Asp	
9741	T	C	Leu	Leu	
10176	A	G	Gln	Gln	
10564	T	A			3′ UTR

[a] The substitution is shown in bold.

TABLE 2. Summary of amino acid changes in clones of the E protein of PL046[a] compared to the consensus sequence

Amino acid position			Frequency
E150	E153	E173	
Ala	Asn	Ala	27/34
Ala	**Glu**	Ala	5/34
Glu	Asn	Ala	1/34
Ala	Asn	**Val**	1/34

[a] The top row represents the consensus sequence; amino acid positions that differed from the consensus are shown in bold.

DISCUSSION

Due to the lack of an appropriate animal model, fundamental questions remain unresolved regarding the role of viral and host factors that contribute to the pathogenesis of human DEN infection. Therefore, the major objective of this study was to

TABLE 3. Summary of amino acid changes in clones of the E protein of D2S10[a] compared to the consensus sequence

Amino acid position								Frequency
E122	E124	E126	E128	E130	E222	E228	E229	
Lys	Asn	Lys	**Glu**	Val	Pro	Gly	Ser	29/43
Lys	**Asp**	Lys	**Glu**	Val	Pro	Gly	Ser	3/43
Lys	Asn	Lys	**Glu**	Val	Pro	**Glu**	Ser	3/43
Ile	Asn	Lys	**Glu**	Val	Pro	Gly	Ser	2/43
Lys	**Ile**	Lys	**Glu**	Val	Pro	Gly	Ser	1/43
Lys	Asn	**Glu**	Lys	Val	Pro	**Glu**	Ser	1/43
Lys	Asn	**Glu**	Lys	Val	Pro	Gly	**Leu**	1/43
Lys	Asn	**Glu**	Lys	Val	Pro	Gly	Ser	1/43
Lys	Asn	Lys	**Glu**	**Met**	Pro	Gly	Ser	1/43
Lys	Asn	Lys	**Glu**	Val	**Ala**	Gly	Ser	1/43

[a] The top row represents the consensus sequence; amino acid positions that differed from the PL046 consensus sequence are shown in bold.

develop a murine model that better resembles human DEN disease. A non-mouse-adapted DEN strain was alternately passaged between mosquito cells and non-neuronal tissues of mice for several rounds to obtain D2S10, a novel DEN strain. Our studies demonstrated that D2S10 was more virulent than the parental strain in mice lacking IFN receptors, causing a lethal but nonparalytic disease in the infected mice. Permeability assays revealed that D2S10 induced increased vascular permeability in several tissues of the infected mice. Immunologic analyses indicated that D2S10-infected mice had high levels of TNF-α in circulation, and treatment of the infected mice with a neutralizing anti-TNF-α Ab prevented early D2S10-induced lethality. Finally, sequence comparisons between D2S10 and the parental DEN strain revealed amino acid charge differences in a conserved region of the E gene, suggesting a role for these particular residues in determining viral virulence and pathogenesis in vivo. Based on these results, D2S10-infected mice represent a more relevant animal model of DEN-induced disease. Moreover, the identification of TNF-α as a key mediator of D2S10-induced disease in mice and the association of viral virulence in vivo with specific amino acid substitutions in the E protein set the foundation for studying the cellular and molecular basis of severe DEN disease in vivo.

Previous studies have shown that sequential series of liver-to-liver passages of YFVs in hamsters led to the generation of viral strains that cause a more lethal disease in hamsters (21, 33, 39). Instead of serial passaging, we performed alternate passaging of DEN between mosquito cells and mice to obtain D2S10, thereby approximating the natural transmission cycle of DEN between mosquitoes and humans. Similar to hamster-passaged YFV, D2S10 was more virulent than the parental PL046 strain, based on the observations that in AG129 mice, (i) high doses of D2S10, but not PL046, caused a lethal infection within 3 to 5 days p.i. and (ii) lower doses of D2S10 induced paralysis more rapidly than did PL046. Viral titers in tissues of D2S10-infected mice, as determined by plaque assay, were not significantly higher than in PL046-infected mice. Additional methods, such as strand-specific real-time RT-PCR, are now required to assess the contribution of viral load in causing the D2S10-induced phenotype.

Several murine models for DEN-induced disease have been reported. They have been created using a variety of mouse strains, including AG129 (16, 30), A/J (15, 29), and SCID (severe combined immunodeficient) mice that have been reconstituted with human cells (2, 4, 20, 37, 38), infected with either mosquito cell culture-passaged DEN or mouse brain-adapted DEN. DEN-infected mice in the great majority of these models exhibited paralysis, and some the infected mice also developed thrombocytopenia. Of note, a recent model using the SCID-human cord blood cell chimeras and subcutaneous inoculation of low-passage clinical isolates showed relevant signs, such as thrombocytopenia and erythema, without manifesting paralysis (4). However, none of the existing models include signs of increased vascular permeability. The cardinal feature of DHF/DSS in humans is the breakdown of vascular integrity, as evidenced by fluid accumulation in the pleural and peritoneal cavities. In D2S10-infected mice, increased vascular permeability was observed in the liver, spleen, and intestine, as assessed by Evans blue extravasation. However, the relevance of our model to human DEN disease is subject to several limitations. For example, the apparent lack of fluid accumulation in pleural and peritoneal cavities of D2S10-infected mice could be due to species differences in the pathogenesis of DEN disease. Alternatively, different manipulations of the virus and host components may be necessary to generate a more suitable murine model of DEN-induced vascular leakage. In particular, a mouse model that requires lower doses of virus and is less immunocompromised than AG129 mice might better reflect natural DEN infection in humans, since a high viral dose, in combination with a deficient IFN-dependent immune response of AG129 mice, may trigger an aberrant antiviral response. Therefore, we have continued our passaging strategy using different virus and mouse strains and are currently searching for new DEN strains that cause a more relevant disease in wild-type mice. Specifically, we are attempting to isolate novel DEN strains that induce DF signs, such as thrombocytopenia and erythema, in a majority of wild-type mice and DHF/DSS signs, such as increased vascular permeability, in a small subset of wild-type mice at later times p.i. Meanwhile, despite these limitations, D2S10-infected AG129 mice provide the first opportunity to investigate the pathogenic mechanism of vascular leakage during DEN infection in vivo.

A major finding of this study is the identification of TNF-α as a critical component of D2S10-induced lethality in AG129 mice. In agreement with studies demonstrating that the sera from patients with DHF/DSS contain greater levels of several proinflammatory cytokines, including TNF-α, than sera from individuals with DF (10, 13, 17), D2S10- but not PL046-infected AG129 mice contain elevated levels of TNF-α in the serum. Neutralization of this cytokine alone was sufficient to decrease the severity of disease in D2S10-infected mice and to delay death significantly. Our result is consistent with a previous study that showed that anti-TNF-α treatment decreased the rate of paralysis in BALB/c mice after infection with mouse brain-adapted DEN (3). Therefore, among all the inflammatory mediators that have been implicated in the pathogenesis of human DEN disease, TNF-α may be one of the major players that modulate the severity of disease. Future experiments, starting with the identification of cellular sources and targets of TNF-α, are now necessary to determine why this cytokine is produced in D2S10-infected animals. Potential explanations for TNF-α induction include higher viral loads and/or more intense inflammatory responses in particular tissues or at certain time points p.i. in D2S10-infected mice compared to those in PL046-infected mice. However, in preliminary Evans blue uptake studies, anti-TNF-α treatment appeared to result in a decrease in vascular permeability in the spleen but not in other tissues of D2S10-infected mice (data not shown), suggesting that different immune effector molecules may be responsible for the breakdown of the vascular integrity in different tissues. Further studies with D2S10-infected AG129 mice at both virologic and immunologic levels should allow us to dissect the mechanisms by which TNF-α and other immune effectors modulate the severity of DEN-induced disease in vivo.

Finally, another major finding of the present study is the identification of potential viral determinants that are likely to mediate the D2S10-specific phenotype described above. At the consensus sequence level, the genomes of D2S10 and PL046 viruses varied by eight nucleotides, with only one amino acid change in domain II of the E protein and one nucleotide

substitution in the 3′ UTR. In vivo selection led to greater nucleotide heterogeneity in the envelope region, based on sequence analysis of clones that span the E protein of PL046 versus D2S10. Consensus sequence analysis of the E region of early mouse passages of D2S10 revealed the amino acid change (K128E) in domain II of the E protein starting at passage 5. Since the D2S10-like phenotype was observed at passage 7, but not at passages 5 and 6, additional sequencing is now needed to determine whether passages 5 and 6 have less heterogeneity than passage 7. We have also sequenced the entire genome of the virus isolated from mesenteric lymph nodes of a D2S10-infected AG129 mouse. At the consensus level, the lymph node virus contains the expected K128E change plus another (N124D) mutation in the E protein. Collectively, our sequence data suggest that this K128E mutation in the E protein is stable. Since the E protein plays a major role in viral tropism (26) and the 3′ UTR is involved in DEN translation and replication (1, 14), these particular mutations in the E protein and the 3′ UTR may be involved in the increased virulence of D2S10. Similarly, few nucleotide changes were associated with the serial passage of YFV in hamsters, and a majority of amino acid changes of the hamster-virulent YFV also occurred in the E protein (21). Taken together, these findings suggest that, at the consensus sequence level, flaviviruses accumulate few mutations in vivo and that these mutations tend to cluster in the E protein. However, within the E protein, the hamster-passaged YFV strain carried mutations in domains I and III, whereas D2S10 contained changes in domain II, suggesting different mechanism of action for the increased virulence of these viruses. Analysis of clones derived from domain II of the E protein of PL046 versus D2S10 implicated several potential mechanisms. First, all eight amino acid changes in D2S10 were localized near the region that is postulated to regulate fusion activity, suggesting a role for viral entry and fusion in D2S10-induced virulence (23). Second, these eight amino acids, which were part of a conserved, basic patch in PL046, converted into negatively charged or uncharged residues in D2S10, potentially disrupting normal interactions between the basic residues and cell surface components such as heparan sulfate (24). Third, the viral diversity in D2S10 was increased compared to that in PL046, and this might indicate a role for the viral population as a whole, as opposed to a specific viral variant, in modulating the D2S10-induced phenotype in vivo (36). Further studies using molecular clones of these viruses are now required to determine the significance of the specific D2S10 mutations. Specifically, we have generated an infectious cDNA clone of PL046 and are currently engineering the particular D2S10-specific mutations into the parental virus.

In conclusion, inoculation of AG129 mice lacking IFN receptors with D2S10, a novel DEN strain that was isolated after alternate passaging between mosquito cells and mice, resulted in a TNF-α-mediated lethal infection. Infected mice manifested increased vascular permeability and lacked signs of paralysis early after infection. Sequence analysis of the parental and D2S10 viruses suggested that a conserved patch of basic residues in domain II of the E protein might be a major target for increasing viral virulence in vivo.

ACKNOWLEDGMENTS

We thank Sondra Schlesinger, Milton Schlesinger, and Michael Diamond at Washington University School of Medicine, St. Louis, Mo., for helpful discussions. We also thank Jennifer Kyle, Scott Balsitis, and Katie Minor for both their technical help and critical insights.

This research was supported by grants ID-IA-0031-02 from the Ellison Medical Foundation and CRA-14 from the Pediatric Dengue Vaccine Initiative (to E.H.) and an LIAI institutional start-up fund (to S.S.).

REFERENCES

1. **Alvarez, D. E., A. L. De Lella Ezcurra, S. Fucito, and A. V. Gamarnik.** 2005. Role of RNA structures present at the 3′UTR of dengue virus on translation, RNA synthesis, and viral replication. Virology **339:**200–212.
2. **An, J., J. Kimura-Kuroda, Y. Hirabayashi, and K. Yasui.** 1999. Development of a novel mouse model for dengue virus infection. Virology **263:**70–77.
3. **Atrasheuskaya, A., P. Petzelbauer, T. M. Fredeking, and G. Ignatyev.** 2003. Anti-TNF antibody treatment reduces mortality in experimental dengue virus infection. FEMS Immunol. Med. Microbiol. **35:**33–42.
4. **Bente, D. A., M. W. Melkus, J. V. Garcia, and R. Rico-Hesse.** 2005. Dengue fever in humanized NOD/SCID mice. J. Virol. **79:**13797–13799.
5. **Brandt, W. E., J. M. McCown, M. K. Gentry, and P. K. Russell.** 1982. Infection enhancement of dengue type 2 virus in the U-937 human monocyte cell line by antibodies to flavivirus cross-reactive determinants. Infect. Immun. **36:**1036–1041.
6. **Burke, D. S., and T. P. Monath.** 2001. Flaviviruses, p. 1043–1126. *In* D. M. Knipe and P. M. Howley (ed.), Fields virology, 4th ed., vol. 1. Lippincott Williams and Wilkins, Philadelphia, Pa.
7. **Cologna, R., P. M. Armstrong, and R. Rico-Hesse.** 2005. Selection for virulent dengue viruses occurs in humans and mosquitoes. J. Virol. **79:**853–859.
8. **Cologna, R., and R. Rico-Hesse.** 2003. American genotype structures decrease dengue virus output from human monocytes and dendritic cells. J. Virol. **77:**3929–3938.
9. **dos Santos, F. B., M. P. Miagostovich, R. M. Nogueira, H. G. Schatzmayr, L. W. Riley, and E. Harris.** 2004. Analysis of recombinant dengue virus polypeptides for dengue diagnosis and evaluation of the humoral immune response. Am. J. Trop. Med. Hyg. **71:**144–152.
10. **Green, S., D. W. Vaughn, S. Kalayanarooj, S. Nimmannitya, S. Suntayakorn, A. Nisalak, R. Lew, B. L. Innis, I. Kurane, A. L. Rothman, and F. A. Ennis.** 1999. Early immune activation in acute dengue illness is related to development of plasma leakage and disease severity. J. Infect. Dis. **179:**755–762.
11. **Halstead, S. B.** 1988. Pathogenesis of dengue: challenges to molecular biology. Science **239:**476–481.
12. **Halstead, S. B., and E. J. O'Rourke.** 1977. Antibody-enhanced dengue virus infection in primate leukocytes. Nature **265:**739–741.
13. **Hober, D., L. Poli, B. Roblin, P. Gestas, E. Chungue, G. Granic, P. Imbert, J. L. Pecarere, R. Vergez-Pascal, P. Wattre, et al.** 1993. Serum levels of tumor necrosis factor-alpha (TNF-alpha), interleukin-6 (IL-6), and interleukin-1 beta (IL-1 beta) in dengue-infected patients. Am. J. Trop. Med. Hyg. **48:**324–331.
14. **Holden, K. L., D. A. Stein, T. C. Pierson, A. A. Ahmed, K. Clyde, P. L. Iversen, and E. Harris.** 2005. Inhibition of dengue virus translation and RNA synthesis by a morpholino oligomer targeted to the top of the terminal 3′ stem-loop structure. Virology **344:**439–452.
15. **Huang, K.-J., S.-Y. J. Li, S.-C. Chen, H.-S. Liu, Y.-S. Lin, T.-M. Yeh, C.-C. Liu, and H.-Y. Lei.** 2000. Manifestation of thrombocytopenia in dengue-2-virus-infected mice. J. Gen. Virol. **81:**2177–2182.
16. **Johnson, A. J., and J. T. Roehrig.** 1999. New mouse model for dengue virus vaccine testing. J. Virol. **73:**783–786.
17. **Kittigul, L., W. Temprom, D. Sujirarat, and C. Kittigul.** 2000. Determination of tumor necrosis factor-alpha levels in dengue virus infected patients by sensitive biotin-streptavidin enzyme-linked immunosorbent assay. J. Virol. Methods **90:**51–57.
18. **Lei, H. Y., T. M. Yeh, H. S. Liu, Y. S. Lin, S. H. Chen, and C. C. Liu.** 2001. Immunopathogenesis of dengue virus infection. J. Biomed. Sci. **8:**377–388.
19. **Leitmeyer, K. C., D. W. Vaughn, D. M. Watts, R. Salas, I. Villalobos de Chacon, C. Ramos, and R. Rico-Hesse.** 1999. Dengue virus structural differences that correlate with pathogenesis. J. Virol. **73:**4738–4747.
20. **Lin, Y. L., C. L. Liao, L. K. Chen, C. T. Yeh, C. I. Liu, S. H. Ma, Y. Y. Huang, Y. L. Huang, C. L. Kao, and C. C. King.** 1998. Study of dengue virus infection in SCID mice engrafted with human K562 cells. J. Virol. **72:**9729–9737.
21. **McArthur, M. A., M. T. Suderman, J. P. Mutebi, S. Y. Xiao, and A. D. Barrett.** 2003. Molecular characterization of a hamster viscerotropic strain of yellow fever virus. J. Virol. **77:**1462–1468.
22. **Meltzer, M. I., J. G. Rigau-Perez, G. G. Clark, P. Reiter, and D. J. Gubler.** 1998. Using disability-adjusted life years to assess the economic impact of dengue in Puerto Rico: 1984–1994. Am. J. Trop. Med. Hyg. **59:**265–271.
23. **Modis, Y., S. Ogata, D. Clements, and S. C. Harrison.** 2003. A ligand-binding pocket in the dengue virus envelope glycoprotein. Proc. Natl. Acad. Sci. USA **100:**6986–6991.
24. **Modis, Y., S. Ogata, D. Clements, and S. C. Harrison.** 2005. Variable surface epitopes in the crystal structure of dengue virus type 3 envelope glycoprotein. J. Virol. **79:**1223–1231.
25. **Mongkolsapaya, J., W. Dejnirattisai, X. N. Xu, S. Vasanawathana, N.**

Tangthawornchaikul, A. Chairunsri, S. Sawasdivorn, T. Duangchinda, T. Dong, S. Rowland-Jones, P. T. Yenchitsomanus, A. McMichael, P. Malasit, and G. Screaton. 2003. Original antigenic sin and apoptosis in the pathogenesis of dengue hemorrhagic fever. Nat. Med. **9:**921–927.

26. **Mukhopadhyay, S., R. J. Kuhn, and M. G. Rossmann.** 2005. A structural perspective of the flavivirus life cycle. Nat. Rev. Microbiol. **3:**13–22.
27. **Rothman, A. L.** 2003. Immunology and immunopathogenesis of dengue disease. Adv. Virus Res. **60:**397–419.
28. **Rothman, A. L., and F. A. Ennis.** 1999. Immunopathogenesis of dengue hemorrhagic fever. Virology **257:**1–6.
29. **Shresta, S., J. L. Kyle, P. Robert Beatty, and E. Harris.** 2004. Early activation of natural killer and B cells in response to primary dengue virus infection in A/J mice. Virology **319:**262–273.
30. **Shresta, S., J. L. Kyle, H. M. Snider, M. Basavapatna, P. R. Beatty, and E. Harris.** 2004. Interferon-dependent immunity is essential for resistance to primary dengue virus infection in mice, whereas T- and B-cell-dependent immunity are less critical. J. Virol. **78:**2701–2710.
31. **Shresta, S., K. L. Sharar, D. M. Prigozhin, H. M. Snider, P. R. Beatty, and E. Harris.** 2005. Critical roles for both STAT1-dependent and STAT1-independent pathways in the control of primary dengue virus infection in mice. J. Immunol. **175:**3946–3954.
32. **Solomon, T., N. M. Dung, D. W. Vaughn, R. Kneen, L. T. Thao, B. Raengsakulrach, H. T. Loan, N. P. Day, J. Farrar, K. S. Myint, M. J. Warrell, W. S. James, A. Nisalak, and N. J. White.** 2000. Neurological manifestations of dengue infection. Lancet **355:**1053–1059.
33. **Tesh, R. B., H. Guzman, A. P. da Rosa, P. F. Vasconcelos, L. B. Dias, J. E. Bunnell, H. Zhang, and S. Y. Xiao.** 2001. Experimental yellow fever virus infection in the golden hamster (Mesocricetus auratus). I. Virologic, biochemical, and immunologic studies. J. Infect. Dis. **183:**1431–1436.
34. **Thompson, L. F., H. K. Eltzschig, J. C. Ibla, C. J. Van De Wiele, R. Resta, J. C. Morote-Garcia, and S. P. Colgan.** 2004. Crucial role for ecto-5′-nucleotidase (CD73) in vascular leakage during hypoxia. J. Exp. Med. **200:**1395–1405.
35. **Vaughn, D. W., S. Green, S. Kalayanarooj, B. L. Innis, S. Nimmannitya, S. Suntayakorn, T. Endy, B. Raengsakulrach, A. L. Rothman, F. A. Ennis, and A. Nisalak.** 2000. Dengue viremia titer, antibody response pattern, and virus serotype correlate with disease severity. J. Infect. Dis. **181:**2–9.
36. **Vignuzzi, M., J. K. Stone, J. J. Arnold, C. E. Cameron, and R. Andino.** 2006. Quasispecies diversity determines pathogenesis through cooperative interactions in a viral population. Nature **439:**344–348.
37. **Whitehead, S. S., B. Falgout, K. A. Hanley, J. E. Blaney, Jr., L. Markoff, and B. R. Murphy.** 2003. A live, attenuated dengue virus type 1 vaccine candidate with a 30-nucleotide deletion in the 3′ untranslated region is highly attenuated and immunogenic in monkeys. J. Virol. **77:**1653–1657.
38. **Wu, S. J., C. G. Hayes, D. R. Dubois, M. G. Windheuser, Y. H. Kang, D. M. Watts, and D. G. Sieckmann.** 1995. Evaluation of the severe combined immunodeficient (SCID) mouse as an animal model for dengue viral infection. Am. J. Trop. Med. Hyg. **52:**468–476.
39. **Xiao, S. Y., H. Zhang, H. Guzman, and R. B. Tesh.** 2001. Experimental yellow fever virus infection in the golden hamster (Mesocricetus auratus). II. Pathology. J. Infect. Dis. **183:**1437–1444.